Ganendra : Majalah IPTEK Nuklir *p-ISSN: 1410-6957, e-ISSN: 2503-5029*
Ganendra : Journal of Nuclear Science and Technology *https://jurnal.batan.go.id/index.php/ganendra*
Vol. 26 No. 1, 2023: 1-8

STUDY OF POISSON NOISE REDUCTION ON GAMMA CAMERA IMAGE USING SPATIAL DOMAIN FILTER

STUDI REDUKSI NOISE POISSON PADA CITRA GAMMA CAMERA MENGGUNAKAN FILTER DOMAIN SPASIAL

Ayu Jati Puspitasari[1,*], Risky Nurseila Karthika[1], Puspa Ayu Nugrahani[1], Widya Febrianti[1], Nur Rahmah Hidayati[2]
[1]Polytechnic Institute of Nuclear Technology – National Research and Innovation Agency, Jl. Babarsari PO BOX 6101 YKBB, Sleman, D. I. Yogyakarta, 55281
[2]Research Center for Safety, Metrology, and Nuclear Quality Technology - National Research and Innovation Agency, Jl. Lebak Bulus Raya, Lb. Bulus, Jakarta Selatan, DKI Jakarta, 12440

*Corresponding author e-mail : ayuj001@brin.go.id

Received 28 February 2023, revised 18 July 2023 , accepted 15 August 2023

ABSTRACT

STUDY OF POISSON NOISE REDUCTION ON GAMMA CAMERA IMAGE USING SPATIAL DOMAIN FILTER. *A gamma camera image is produced by a gamma camera that detects the gamma radiation emitted by the radioactive substance or radiopharmaceutical injected into the body. The gamma camera image sometimes has noise that can interfere with the diagnosis. This image is commonly affected by a Poisson-type random noise. This research proposes using a spatial domain filter to study Poisson noise reduction in gamma camera images. The image sample used is the image of a mouse injected with Lu-177-DOTA Trastuzumab with 100 µCi activity detected using a dual-head gamma camera with NaI(Tl) detectors. The grayscale image is treated with Poisson noise, then improved using a spatial domain filter. The spatial domain filters used include Mean, Median, Wiener, and Spatial Lowpass Filters. The mean filter is the best one that can reduce Poisson noise among the four applied filters. The best filter size for noise reduction is 3 with MSE 5.07, PSNR 41.08 dB, and SSIM 0.99.*

Keywords*: gamma camera image, noise reduction, poisson noise, spatial domain filter*

ABSTRAK

STUDI REDUKSI NOISE POISSON PADA CITRA GAMMA CAMERA MENGGUNAKAN FILTER DOMAIN SPASIAL. *Citra kamera gamma dihasilkan oleh kamera gamma yang mendeteksi emisi radiasi gamma hasil dari injeksi zat radioaktif atau radiofarmaka ke dalam tubuh. Citra kamera gamma yang dihasilkan terkadang memiliki noise yang dapat mengganggu diagnosis. Citra ini biasanya dipengaruhi oleh noise acak tipe Poisson. Penelitian ini bertujuan untuk mengurangi noise Poisson pada citra kamera gamma menggunakan filter domain spasial. Sampel citra yang digunakan adalah citra tikus yang diinjeksi Lu-177-DOTA Trastuzumab dengan aktivitas 100 µCi yang dideteksi menggunakan kamera gamma dual head dengan detektor NaI(Tl). Citra grayscale diberi noise Poisson, kemudian dilakukan reduksi noise menggunakan filter domain spasial. Filter domain spasial yang digunakan antara lain Filter Mean, Median, Wiener, and Spatial Lowpass. Filter Mean adalah filter terbaik yang dapat mereduksi noise Poisson dibanding keempat filter lainnya. Ukuran filter terbaik untuk mereduksi noise adalah ukuran 3 dengan MSE 5,07, PSNR 41,08 dB, dan SSIM 0,99.*

Kata kunci*: citra kamera gamma, pengurangan noise, poisson noise, filter domain spasial*

INTRODUCTION

Nuclear medicine is a medical specialty that uses radioactive or radiopharmaceuticals in the human body in-vivo or in-vitro for diagnostic or therapeutic purposes. The radioactive or radiopharmaceuticals get into the patient's body through inhalation, ingestion, and injection. Diagnostic nuclear medicine principally assesses organ function (physiology or pathophysiology). A gamma camera is utilized to detect and quantify the radiopharmaceuticals' in-vivo biodistribution. The essential parts of the gamma camera consist of the collimator, scintillator, photomultiplier tube (PMT), and position logic circuit [1]–[5]. The two kinds of gamma cameras that are SPECT (Single Photon Emission Computed Tomography) and planar gamma cameras, have a difference in that planar produces a 2D

https://doi.org/10.55981/gnd.2023.6822

image, and SPECT generates a 3D image [3], [6]. Planar scintigraphy or planar gamma camera images the spreading of radioactive substance in a 2D image. These are mainly used for whole-body examinations [7].

The factors determining nuclear image quality are contrast, noise, and spatial resolution. Radioactive imaging is an intrinsically noisy examination. Excessive noise can weaken the detection of an object, especially if the object has low contrast. One of the formed noises is affected by the non-uniformity of the gamma camera. The random type of noise can be influenced by statistical noise or random variations in count density due to the spontaneous activity of radioactive decay [8]. Gamma camera images are generally disturbed by Poisson-type random noise, which reduces the image qualitatively and quantitatively and becomes an intervening factor for degradation [9]. Poisson noise (shot noise) is an electronic noise that arises when the number of photons or electrons is insignificant enough to cause detectable statistical fluctuations in measurement and follow the Poisson distribution [10]–[12]. Because this signal is nature-dependent, standard noise reduction techniques cannot be used. One of the well-known filter algorithms for removing Poisson noise is the spatial domain filter [11].

The spatial domain filter reduces Poisson noise in this study. The spatial domain plays an essential role due to the use of gamma camera detectors. A spatial Domain Filter is a filter that works with the convolution method. A spatial domain filter forms a spatial window to evaluate each pixel value in a digital image. The mechanism of the spatial domain filter is to form a square window or filter, mask, filter mask, kernel, or odd-sized template, such as pixel size 3, 5, 7, and so on [13] as seen in Figure 1.

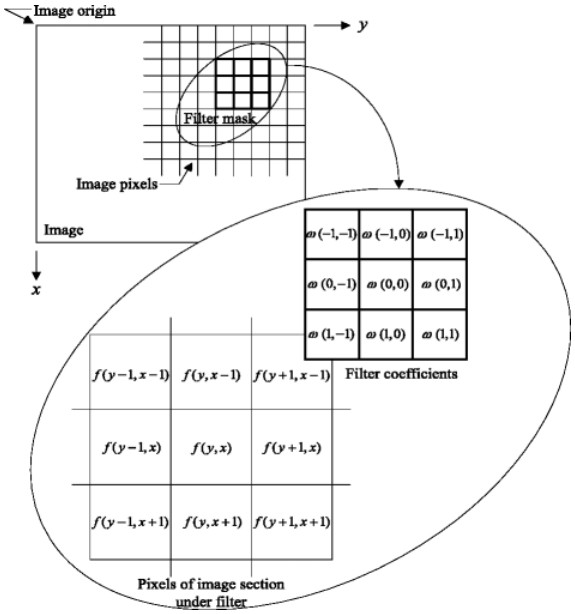

Figure 1. The mechanics of spatial filter using a 3 × 3 mask [14]

In this study, the gamma camera images treated by Poisson noise are reduced by median, spatial lowpass, mean, and wiener filters [15]–[17]. The Mean Filter is a linear filter that applies a mask to each pixel in the signal. It involves averaging the components of the pixels that fall under the mask, resulting in a single pixel value. Subsequently, this newly calculated pixel value is utilized to replace the corresponding pixel in the original signal [18]. The median refers to the middle value in a sorted list of numbers. When the list has an odd count, there is one unique median value. However, if the count is even, there may be multiple center values. It is recommended to use odd list sizes when searching for a median. The Median Filter involves sorting the magnitudes of vectors within a mask to perform the filtering process [18]. Spatial Lowpass filter is a filter that extracts low-frequency image data while discarding or attenuating high frequencies. Lowpass filters are used to achieve blur or smoothing effects and noise reduction. The characteristics of a lowpass filter kernel include all positive values and the sum of all values equal to 1 (one) [16]. The Wiener filter is used to reduce noise in signals. This filter minimizes the mean square error between the estimated process and the desired process. This is done to minimize the overall mean square error in the inverse filtering and noise smoothing process. Filters are generally used to eliminate additive noise. The main objective of the Wiener filter is to reduce the Mean Square Error (MSE) value [17].

Noise reduction program using Python programming language [19]. After filtering, the quality of the filter will be evaluated using MSE (mean square error), PSNR (peak signal-to-noise ratio), and SSIM (structure similarity index measure) [20]–[24].

 https://doi.org/10.55981/gnd.2023.6822

The Mean Squared Error (MSE) is a widely used parameter for quantifying image quality. It computes the average of the squared cumulative errors between the resulting and original images, with values closer to zero indicating better quality [8, 21]. Peak Signal-to-Noise Ratio (PSNR) is a measure of the quality of a reconstructed signal. It is defined as the ratio between the maximum possible power value of a signal and the strength of the noise affecting the image [26]. To calculate PSNR, MSE must be calculated first [24]. The equations for MSE and PSNR are represented by Eq. (1) and Eq. (2), respectively.

$$MSE = \frac{1}{m \times n} \sum_{i=0}^{m-1} \sum_{j=0}^{n-1} [I(i,j) - K(i,j)]^2 \quad (1)$$

$$PSNR = 10 \log_{10} \left(\frac{MAX_I^2}{MSE} \right) = 20 \log_{10} \left(\frac{MAX_I}{\sqrt{MSE}} \right) = 20 \log_{10}(MAX_I) - 10 \log_{10}(MSE) \quad (2)$$

In this context, $I\ (i,j)$ represents the original image, $K\ (i,j)$ denotes the reconstructed image, and m, n represent the pixel dimensions of the image. MAX_I represents the maximum pixel value achievable in the image, and MSE corresponds to the Mean Square Error [26].

The Structure Similarity Index Measure (SSIM) is a methodological algorithm for comparing the structural features of images, where image quality is described in terms of structural similarity. Prior to utilizing SSIM for image quality assessment, a reference image is required. Subsequently, the experimental image and the reference image are juxtaposed to measure their structural similarity. Higher similarity indicates higher quality of the resulting image, while lower similarity corresponds to lower image quality [21]. The SSIM algorithm separates the features of luminance, contrast, and structure from two signals, then compares these features and obtains an equation through their combination. The SSIM index is determined using the following equation (3) [27].

$$SSIM(x,y) = \frac{(2\mu_x\mu_y + C_1)(2\sigma_{xy} + C_2)}{(\mu_x{}^2 + \mu_y{}^2 + C_1)(\sigma_x{}^2 + \sigma_y{}^2 + C_2)} \quad (3)$$

The μ_x and μ_y denote the means of the two original images with their respective references, σ_x and σ_y represent the standard deviations of the two original images with their respective references, and C_1 and C_2 are constants [27].

METHODOLOGY

The test image used in this study is Mediso AnyScan S Dual Head medical gamma camera image with a NaI(Tl) detector. The test image is the result of imaging the mouse as an object as an RGB format image (.jpg) with an image size of 953 × 109 pixels [28]. The mouse was used as three images as samples for research material after being injected with radioactive Lu177 – DOTA Trastuzumab with 100 µCi activity. The mouse images were varied based on the time Lu-177 had been in the mouse's body for 69, 21, and 0 hours. The time points 69, 21, and 0 hours show the process of Lu-177 absorption in the mouse's body. Figure 2 shows the initial images.

(a) (b) (c)

Figure 2. Initial images: Lu-177 time absoption: (a) 69 hours; (b) 21 hours; and (c) 0 hours

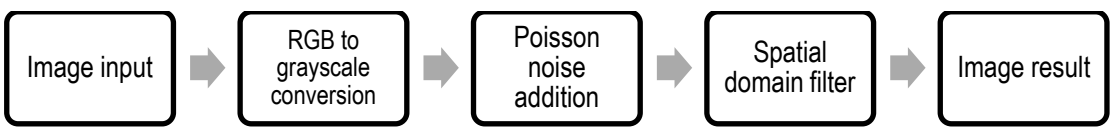

Figure 3. The flowchart of the program

The flowchart of the program is shown in Figure 3. The RGB image first converted to a grayscale image with the scikit-image feature. Furthermore, the grayscale image is added by Poisson Noise with a noise density of 20. The noise is set at a sufficiently high level to consider the effectiveness of the filters used. The addition of Poisson

noise aims to determine differences in the image before and after denoising. After adding Poisson Noise to the gamma camera image with the mouse sample, the next step is image reduction using the spatial domain filter method, which includes the mean filter, median filter, wiener filter, and spatial lowpass filter. Noised images will then be filtered with several variations of filter sizes 3, 5, 7, 9, and 11. The selection of matrix size is based on utilizing odd-sized matrices to account for the image convolution process. Furthermore, the reduced image samples are tested based on the values of MSE (mean square error), PSNR (peak signal-to-noise ratio), and SSIM (structure similarity index measure) to determine the quality of the image after being filtered using the spatial domain filter.

RESULTS AND DISCUSSIONS

Three samples of mouse images were used with different radioactive injection times at 69, 21, and 0 hours. Among the three images, it can be obtained that the longer the duration of injection time, the sharper the resulting image. It is because the longer the duration of injection time, the more gamma emission radiation that is injected is emitted and spreads throughout the mouse's body. Data collection is established in noise reduction with mean, median, wiener, and spatial lowpass filters with filter size variations of 3, 5, 7, 9, and 11. Figure 4 (a) (b) and (c) below are the results of mouse images with a radioactive injection time of 69 hours, 21 hours, and 0 hours which the mean filter has reduced.

(a) (b) (c)

Figure 4. (a) Results of mean filter reduced mouse image with duration of injection time 69 hours; (b) 21 hours; (c) 0 hours

Figure 5 (a) (b) and (c) below are the results of mouse images with a radioactive injection time of 69 hours; 21 hours; and 0 hours which has been reduced by the median filter.

(a) (b) (c)

Figure 5. (a) Results of median filter reduced mouse image with duration of injection time 69 hours; (b) 21 hours; (c) 0 hours

Figure 6 (a) (b) and (c) below are the results of mouse images with a radioactive injection time of 69 hours; 21 hours; and 0 hours which has been reduced by the wiener filter.

(a) (b) (c)

Figure 6. (a) Results of wiener filter reduced mouse image with duration of injection time 69 hours; (b) 21 hours; (c) 0 hours

https://doi.org/10.55981/gnd.2023.6822

Figure 7 (a) (b) and (c) below are the results of mouse images with a radioactive injection time of 69 hours; 21 hours; and 0 hours which has been reduced by the spatial lowpass filter.

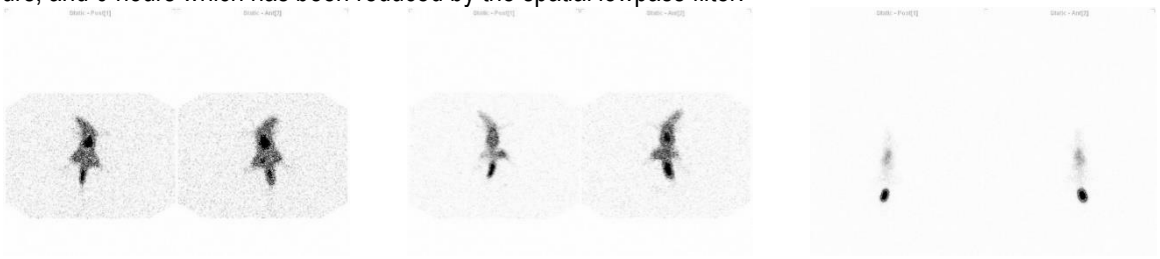

(a) (b) (c)

Figure 7. (a) Results of spatial low pass filter reduced mouse image with duration of injection time 69 hours; (b) 21 hours; (c) 0 hours

There are three types of mouse images used based on the Lu-177 uptake time, which are 69 hours, 21 hours, and 0 hours. A mouse was injected with Lu-177 in its tail. In Figure 4-7 (c), it can be observed that the radioactive substance accumulates in the tail. As time progresses, the radioactive substance spreads throughout the mouse's body (Figure 4-7 (b)). In Figure 4-7 (a), the distribution of the radioactive substance continues to spread and is absorbed throughout the mouse's body, with radiation scatter observed around the outer surface of the mouse's body.

If observed visually, the noise resulting from the reduced image is difficult to detect, so a test is carried out using the parameter values of the MSE (mean square error), PSNR (peak signal-to-noise ratio), and SSIM (structure similarity index measure) shown in Table 1.

The quality of the denoising image filter is then evaluated using the MSE, PSNR, and SSIM values. The MSE is a measurement of the quality in an estimator. MSE is not able to be distinguished visually. MSE displays the difference between the reconstructed vector image and the reference image. A low MSE value indicates that both vectors are equal [29]. It is always non-negative, and the values close to zero are better [30]. The best MSE value based on the test results data is shown on the mean and spatial lowpass filter, which equals 5.07. MSE is also known as noise power, a small value indicates that the image's noise is slight.

The high PSNR value is also shown in the mean and spatial lowpass filter, equal to 41.08 dB for 0 hours of injection duration. A higher PSNR value provides a higher image quality [31]. Fatma Makhlouf et al. (2013) did related research using scintigraphy images. The wavelet transformation that has been done reduces the Poisson noise of a scintigraphic image, with average PSNR results of 32.21 dB [9]. Thus, the image results in this study based on 0 hours of injection time in mean and spatial lowpass filters are better.

The following image quality test parameter is SSIM. The SSIM measures distortions in combination with loss of correlation, distortion of luminance and distortion of contrast. The range is 0-1, where the best value of SSIM is 1 [32]. The best SSIM value is also found in the mean and spatial lowpass filter results, which is 0.99.

Both of these filters, mean and spatial lowpass filters, have almost the same image quality in all evaluation parameters. However, this slight difference can be seen in the 21-hour images. The SSIM of the 21-hour image on the mean filter is higher than the lowpass spatial filter, which is 0.98. Based on the results in the table, among the four filters, the best filter for noise reduction is the mean filter because it has the lowest MSE value, the highest PSNR value, and the closest SSIM to 1.

Among the data of the four filters, the best image based on the duration of injection time is 0 hours image. This is because the radioactive substance is still collected in the tail of a mouse and has not spread to the body, so the scattering of gamma radiation is relatively small.

Considering the resolution image, the image used is quite good, with a size of 953 × 109 pixels. The higher the image resolution or the bigger the image size, the better the image quality [33]. For all filters, the best image is produced by a filter size of 3. The image is blurred when the filter size increases [34]. A larger filter size has more values to calculate into the average, meaning a larger filter size blurs the image more than a smaller one [35]. This will increase the MSE value, but PSNR and SSIM will decrease.

Table 1. Results of testing the reduced image with four types of spatial domain filters based on MSE, PSNR, and SSIM value

Filter	Duration of Injection Time											
	69 hours				21 hours				0 hours			
Mean	**Filter size**	**MSE**	**PSNR (dB)**	**SSIM**	**Filter size**	**MSE**	**PSNR (dB)**	**SSIM**	**Filter size**	**MSE**	**PSNR (dB)**	**SSIM**
	3	**30.09**	**33.35**	**0.96**	**3**	**14.15**	**36.62**	**0.98**	**3**	**5.07**	**41.08**	**0.99**
	5	55.33	30.70	0.89	5	25.69	34.03	0.94	5	7.41	39.44	0.99
	7	73.41	29.47	0.83	7	33.82	32.84	0.91	7	9.23	38.48	0.99
	9	83.48	28.92	0,81	9	38.34	32.29	0.90	9	10.23	38.03	0.98
	11	89.41	28.62	0.79	11	41.2	31.98	0.89	11	10.8	37.79	0.98
Filter	**Duration of Injection Time**											
	69 hours				**21 hours**				**0 hours**			
Median	**Filter size**	**MSE**	**PSNR (dB)**	**SSIM**	**Filter size**	**MSE**	**PSNR (dB)**	**SSIM**	**Filter size**	**MSE**	**PSNR (dB)**	**SSIM**
	3	**30.88**	**33.23**	**0.96**	**3**	**14.46**	**36.53**	**0.98**	**3**	**5.08**	**41.07**	**0.99**
	5	57.13	30.56	0.9	5	26.37	33.92	0.94	5	7.42	39.43	0.99
	7	78.09	29.21	0.84	7	35.87	32.58	0.91	7	10.20	38.05	0.99
	9	88.81	28.65	0,81	9	40.38	32.07	0.90	9	11.13	37.66	0.99
	11	94.58	28.37	0.79	11	42.88	31.81	0.90	11	11.41	37.56	0.99
Filter	**Duration of Injection Time**											
	69 hours				**21 hours**				**0 hours**			
Weiner	**Filter size**	**MSE**	**PSNR (dB)**	**SSIM**	**Filter size**	**MSE**	**PSNR (dB)**	**SSIM**	**Filter size**	**MSE**	**PSNR (dB)**	**SSIM**
	3	**481.13**	**21.31**	**0.93**	**3**	**316.97**	**23.12**	**0.95**	**3**	**187.43**	**25.4**	**0.98**
	5	711.58	19.61	0.84	5	506.68	21.08	0.91	5	331.31	22.93	0.98
	7	813.46	19.03	0.78	7	595.99	20.38	0.88	7	400.21	22.11	0.98
	9	916.75	18.51	0,75	9	698.08	19.69	0.86	9	494.04	21.19	0.96
	11	1027.08	18.01	0.74	11	812.32	19.03	0.86	11	605.67	20.31	0.96
Filter	**Duration of Injection Time**											
	69 hours				**21 hours**				**0 hours**			
Spatial Lowpass	**Filter size**	**MSE**	**PSNR (dB)**	**SSIM**	**Filter size**	**MSE**	**PSNR (dB)**	**SSIM**	**Filter size**	**MSE**	**PSNR (dB)**	**SSIM**
	3	**30.09**	**33.35**	**0.96**	**3**	**14.15**	**36.62**	**0.94**	**3**	**5.07**	**41.08**	**0.99**
	5	55.33	30.7	0.89	5	25.69	34.03	0.94	5	7.41	39.44	0.99
	7	73.41	29.47	0.83	7	33.82	32.84	0.91	7	9.23	38.48	0.99
	9	83.48	28.92	0,81	9	38.34	32.29	0.91	9	10.23	38.03	0.99
	11	89.41	28.62	0.79	11	41.2	31.98	0.89	11	10.8	37.79	0.99

https://doi.org/10.55981/gnd.2023.6822

CONCLUSION

The mean, median, weiner, and spatial lowpass filters applied to gamma camera images can reduce the Poisson noise. The mean filter with filter size 3 is the best with MSE 5.07, PSNR 41.08 dB, and SSIM 0.99. The implementation of a spatial domain filter demonstrates its efficacy in diminishing noise on the gamma camera. However, further enhancements are required to minimize the mean square error (MSE) value, aiming for near-zero levels. Exploring alternative approaches, such as employing a frequency domain filter, may prove beneficial in this endeavor.

ACKNOWLEDGEMENT

The authors would like to acknowledge the Electronic Instrumentation Study Program, Polytechnic Institute of Nuclear Technology for assistance or encouragement, and the Research Center for Safety, Metrology, and Nuclear Quality Technology - National Research and Innovation Agency for providing research data.

REFERENCES

[1] J. Wheat, G. Currie, R. Davidson, and H. Kiat, "An introduction to nuclear medicine," *Radiographer*, vol. 58, no. 3, pp. 38–45, Sep. 2011, doi: 10.1002/J.2051-3909.2011.TB00154.X.

[2] Y. Sasaki and K. Kusakabe, "Nuclear medicine for diagnosis and treatment," *IAEA Off. Public Inf. Commun.*, vol. 17, no. 1, pp. 7–8, 2017.

[3] D. H. Skuldt, *Nuclear medicine*. Vienn: International Atomic Energy Agency, 2014.

[4] F. Kharfi, "Principles and Applications of Nuclear Medical Imaging: A Survey on Recent Developments," *Imaging Radioanal. Tech. Interdiscip. Res. - Fundam. Cut. Edge Appl.*, no. March 2013, 2013, doi: 10.5772/54884.

[5] F. Yang, K. Yang, and C. Yang, "Development and Application of Gamma Camera in the Field of Nuclear Medicine," *Int. J. Sci.*, vol. 4, no. 07, pp. 21–24, 2018, doi: 10.18483/ijsci.1758.

[6] T. Lewellen, "The Scintillation Camera : Planar and SPECT List of Nuclear Medicine 'Single Photon' Radionuclides." Department of Radiology, University of Washington, 2007.

[7] N. B. Smith and A. Webb, *Introduction to Medical Imaging*, 1st editio. Cambridge, England: Cambridge University Press, 2010.

[8] "NM image quality - Radiology Cafe." https://www.radiologycafe.com/frcr-physics-notes/molecular-imaging/nm-image-quality/ (accessed Sep. 23, 2022).

[9] F. Makhlouf, H. Besbes, N. Khalifa, C. Ben Amar, and B. Solaiman, "Planar Scintigraphic Images Denoising," *Open J. Med. Imaging*, vol. 03, no. 04, pp. 116–124, 2013, doi: 10.4236/ojmi.2013.34019.

[10] M. Avinash Shrivastava, P. Bisen, M. Dubey, and M. Choudhari, "Image Denoising Using Different Filters (A Comparison of Filters)," *Int. J. Emerg. Trends Sci. Technol.*, vol. 02, no. 04, pp. 2214–2219, Accessed: Feb. 16, 2023. [Online]. Available: www.ijetst.in.

[11] K. V Thakur, O. H. Damodare, and A. M. Sapkal, "Poisson Noise Reducing Bilateral Filter," *Procedia Comput. Sci.*, vol. 79, pp. 861–865, 2016, doi: 10.1016/j.procs.2016.03.087.

[12] I. R. Ansari, "Image Denoising Using Spatial Domain Filters," *International Journal of Advanced Technology in Engineering and Science*, vol. 1, no. 02, pp 42-53, 2013.

[13] M. H. Oceandra, "Pengurangan Noise Pada Citra Digital Menggunakan metode Statistik Mean, Median, Kombinasi, dan Rekrusif Filter," 2013.

[14] P. Li, X. Liu, and H. Xiao, "Quantum Image Weighted Average Filtering in Spatial Domain," *Int. J. Theor. Phys.*, vol. 56, pp. 1–27, Nov. 2017, doi: 10.1007/s10773-017-3533-1.

[15] B. Yuwono, "Image Smoothing Menggunakan Mean Filtering, Median Filtering, Modus Filtering Dan Gaussian Filtering," *Telematika*, vol. 7, no. 1, 2015, doi: 10.31315/telematika.v7i1.416.

[16] K. Purwanto, A. Bejo, and A. Suwastono, "Implementasi Algoritme High Pass Filter pada FPGA menggunakan Sensor NIOS II," in *Seminar Nasional Inovasi dan Aplikasi Teknologi di Industri*, 2017, pp. 1–5.

[17] A. P., F. K., and A. Krishnan, "An Overview of Mammogram Noise And Denoising Techniques," *Int. J. Eng. Res. Gen. Sci.*, vol. 4, no. 2, pp. 557–563, 2016, doi: 10.1109/MPOT.2015.2396533.

[18] J. C. Church, Y. Chen, and S. V. Rice, "A Spatial Median Filter for noise removal in digital images," *Conf. Proc. - IEEE SOUTHEASTCON*, no. August, pp. 618–623, 2008, doi: 10.1109/SECON.2008.4494367.

[19] JUD, *Pemrograman Python untuk Pemula*. CV Jubilee Solusi Enterprise, 2016.

[20] U. Sara, M. Akter, and M. S. Uddin, "Image Quality Assessment through FSIM, SSIM, MSE and PSNR—A Comparative Study," *J. Comput. Commun.*, vol. 07, no. 03, pp. 8–18, 2019, doi: 10.4236/jcc.2019.73002.

[21] G. Chen, Y. Shen, F. Yao, P. Liu, and Y. Liu, "Region-based moving object detection Using SSIM," *Proc. 2015 4th Int. Conf. Comput. Sci. Netw. Technol. ICCSNT 2015*, pp. 1361–1364, Jun. 2016, doi: 10.1109/ICCSNT.2015.7490981.

[22] X. Wang, "A Coiflets-Based Wavelet Laplace Method for Solving the Riccati Differential Equations," *J. Appl. Math.*, vol. 2014, no. Vim, 2014, doi: 10.1155/2014/257049.

[23] "Image quality and quality control in diagnostic nuclear medicine," *International Atomic Energy Agency*, 2021. https://www.iaea.org/resources/rpop/health-professionals/nuclear-medicine/diagnostic-nuclear-medicine/image-quality-and-quality-control#4 (accessed Apr. 26, 2021).

[24] M. Manju, P. Abarna, and S. Yamini, "Peak Signal to Noise Ratio & Mean Square Error calculation for various Images using the lossless Image compression in CCSDS algorithm," in *International Journal of Pure and Applied Mathematics*, 2018, vol. 119, no. 12, pp. 14471–14477.

[25] M. Nabih, "Time-Frequency analysis of Different types of signals," Ain Shams University, 2016.

[26] A. Dixit and S. Majumdar, "COMPARATIVE ANALYSIS OF COIFLET AND DAUBECHIES WAVELETS USING GLOBAL THRESHOLD FOR IMAGE DENOISING," *Int. J. Adv. Eng. Technol.*, no. November, pp. 2247–2252, 2013.

[27] Z. Wang, A. C. Bovik, H. R. Sheikh, and E. P. Simoncelli, "Image quality assessment: From error visibility to structural similarity," *IEEE Trans. Image Process.*, vol. 13, no. 4, pp. 600–612, Apr. 2004, doi: 10.1109/TIP.2003.819861.

[28] N. R. Hidayati *et al.*, "STUDI AWAL ESTIMASI DOSIS INTERNAL 177Lu-DOTA TRASTUZUMAB PADA MANUSIA BERBASIS UJI BIODISTRIBUSI PADA MENCIT," *urnal Sains dan Teknol. Nukl. Indones.*, vol. 16, no. 02, pp. 105–116, 2015.

[29] A. K. Moorthy, Z. Wang, and A. C. Bovik, "Visual Perception and Quality Assessment," in *Optical and Digital Image Processing: Fundamentals and Applications*, G. Cristobal, P. Schelkens, and H. Thienpont, Eds. New Jersey: John Wiley & Sons, 2011, pp. 419–439.

[30] M. Ali, B. Younes, and A. Jantan, "Image Encryption Using Block-Based Transformation Algorithm," vol. 8, no. February, pp. 11–18, 2008.

[31] A. Horé and D. Ziou, "Image quality metrics: PSNR vs. SSIM," *Proc. - Int. Conf. Pattern Recognit.*, pp. 2366–2369, 2010, doi: 10.1109/ICPR.2010.579.

[32] P. Ndajah, H. Kikuchi, M. Yukawa, H. Watanabe, and S. Muramatsu, "SSIM image quality metric for denoised images," *Int. Conf. Vis. Imaging Simul. - Proc.*, no. November, pp. 53–57, 2010.

[33] A. J. Puspitasari, I. C. Ningsih, M. S. Ridwan, and H. Hamadi, "PLANAR SCINTIGRAPHY IMAGE DE-NOISING USING COIFLET WAVELET," *GANENDRA Maj. IPTEK Nukl.*, vol. 24, no. 2, pp. 75–83, Nov. 2021, Accessed: Feb. 15, 2023. [Online]. Available: https://jurnal.batan.go.id/index.php/ganendra/article/view/6280.

[34] K. Raju, L. Kumar, M. Kumar, and V. K. .R, "Image Denoising using Filters with Varying Window Sizes: A Study," *Int. J. Curr. Trends Eng. Res.*, vol. 2, no. 7, pp. 48–53, 2016, [Online]. Available: https://www.researchgate.net/publication/339106209_Image_Denoising_using_Filters_with_Varying_Window_Sizes_A_Study.

[35] "Blurring Images – Image Processing with Python." https://datacarpentry.org/image-processing/06-blurring/ (accessed Feb. 27, 2023).